



Exploration and determination of the redox properties of the pseudopterosin class of marine natural products

Wei Zhong, R. Daniel Little*

Department of Chemistry & Biochemistry, University of California, Santa Barbara, CA 93106, USA

ARTICLE INFO

Article history:

Received 28 July 2009

Received in revised form 20 August 2009

Accepted 7 September 2009

Available online 11 September 2009

Keywords:

Electron transfer

Redox

Oxidation

Pseudopterosins

Marine natural products

Voltammetry

Adenosine receptors

ABSTRACT

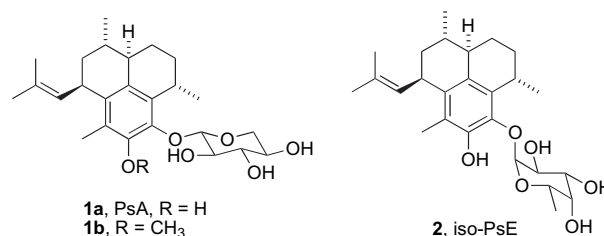
We describe herein the redox chemistry of the pseudopterosin class of marine natural products. Known for their anti-inflammatory and wound healing properties, their chemistry has largely gone unexplored. Details of both voltammetric and preparative scale experiments are provided and speculation is provided concerning the potential role of electron transfer chemistry in the expression of pseudopterosin bioactivity.

© 2009 Elsevier Ltd. All rights reserved.

1. Introduction

The pseudopterosins constitute a class of diterpene glycosides isolated from the marine octocoral *Pseudopterogorgia elisabethae*.^{1–3} They are structurally quite simple molecules, consisting of a tricyclic hydrocarbon core possessing four stereocenters, and a sugar, that is appended to a catechol subunit. Pseudopterosin A (PsA, **1a**), a potent inhibitor of phorbol myristate acetate (PMA)-induced topical inflammation in mice,⁴ stabilizes cell membranes,⁵ prevents the release of prostaglandins and leukotrienes from zymosan stimulated murine macrophages, and inhibits degranulation of human polymorphonuclear leukocytes⁶ and also inhibits phagosome formation in *Tetrahymena* cells.⁷ Its C-10 *O*-methyl ether, **1b**, offers a promising treatment for contact dermatitis,⁸ and displays potent anti-inflammatory and wound healing properties.⁹ In addition to interest in their bioactivity profiles, the pseudopterosins have attracted a significant amount of attention by those persons expert in the art of organic synthesis.¹⁰

Given the presence of the electron rich catechol subunit, it is reasonable to speculate that redox chemistry might play a role in the expression of pseudopterosin bioactivity. In this manuscript, we detail for the first time, their redox behavior under both analytical



(cyclic voltammetry) and preparative scale conditions, characterize the products, examine the anti-inflammatory activity of one of the products derived from iso-PsE (**2**), and speculate concerning the role of redox chemistry in activation of adenosine receptors.^{11,12}

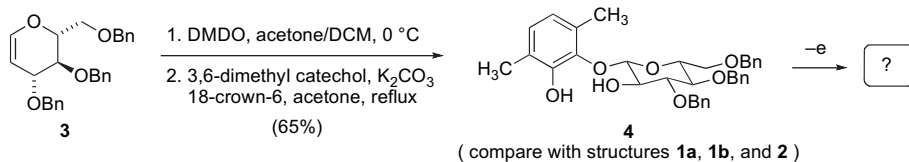
2. Results and discussion

2.1. Cyclic voltammetry

We began conservatively, electing to focus upon **4**, a simplified system that was designed to model the pseudopterosin framework. It was constructed by treating tri-*O*-benzyl-D-glucal (**3**) with DMDO, followed by ring opening of the resulting epoxide using 3,6-dimethyl catechol in the presence of potassium carbonate and 18-crown-6. With **4** in hand, we examined its redox properties voltammetrically.

* Corresponding author. Tel.: +1 805 893 3693; fax: +1 805 893 4120.

E-mail address: little@chem.ucsb.edu (R.D. Little).



As Figure 1 shows, an irreversible wave appeared, displaying a peak potential, E_p , of approximately +1.6 V (Ag/AgNO₃ reference electrode, scan rate 100 mV/s). This value agrees well with those reported in the literature for a variety of substituted catechols.¹³ That the voltammogram displayed an irreversible behavior indicates that the intermediate formed in the oxidation step undergoes a chemical transformation that removes it from the redox equilibrium at a rate that exceeds that of the scan.¹⁴

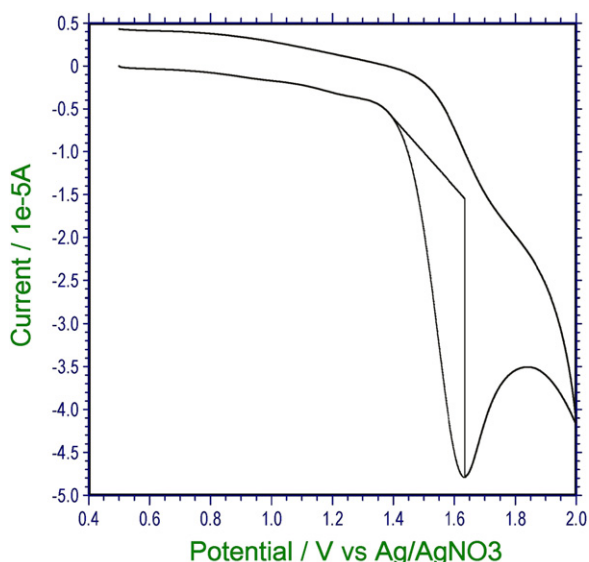
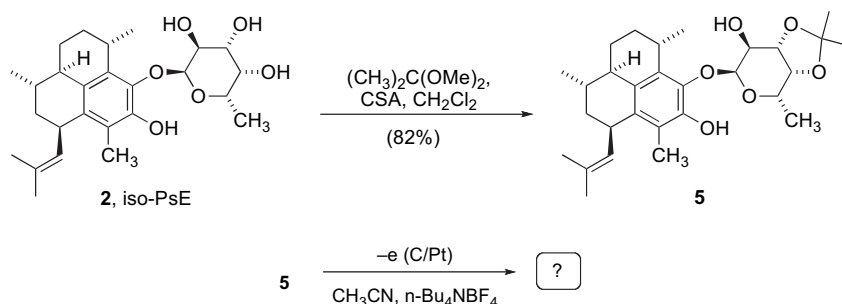


Figure 1. Cyclic voltammogram for model structure **4**: glassy carbon anode, Pt cathode, 100 mV/s scan rate, CH₃CN solvent, 0.1 N (n-Bu)₄NBF₄ supporting electrolyte.

Encouraged by these results, we proceeded to investigate the iso-PsE derived analog **5**. It was constructed by treating iso-PsE (**2**) with acetone dimethyl acetal and CSA. Like the model system **4**, structure **5** also displayed an irreversible redox curve ($E_p \sim 1.5$ V vs Ag/AgNO₃, scan rate 500 mV/s; note Fig. 2), thereby demonstrating that the initially formed cation radical undergoes a follow-up reaction at a rate that exceeds that of the reverse scan.^{15,16} Once again, this begs the question: What is the nature of the transformation(s) that occur after the initial oxidation?



2.2. Preparative scale oxidation; product identification

To address this query each substrate, **4** and **5**, was subjected to a preparative scale oxidation. Phenyliodoso diacetate (PIDA) was pretreated with TFA at 0 °C to generate an equilibrium mixture of

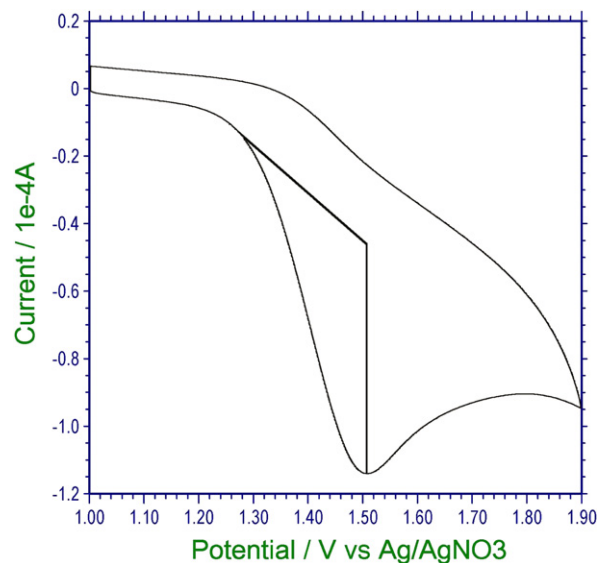


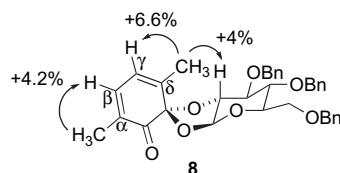
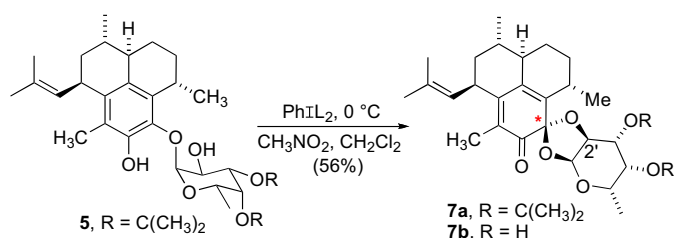
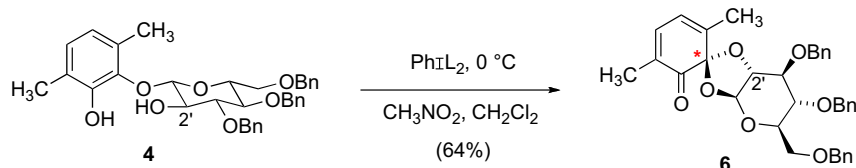
Figure 2. Cyclic voltammogram for iso-PsE derivative, structure **5**: glassy carbon anode, Pt cathode, 500 mV/s scan rate, CH₃CN solvent, 0.1 N (n-Bu)₄NBF₄ supporting electrolyte.

PIDA and its trifluoroacetate analog, PIFA, prior to the dropwise addition of the starting material.^{13,17,18} In the following discussion, we abbreviate the reagent generated in the equilibrium with the symbol PhIL₂, with L referring to both acetate and trifluoroacetate.

Each substrate was transformed to a keto ketal wherein the C-2' hydroxyl group appended to the sugar cyclized onto the aromatic framework, in one case transforming the model system **4** to structure **6**, and in the other converting the natural product derived framework **5** into keto ketal **7a**. In neither instance were we able to detect the formation diastereomers at the newly formed stereocenter (marked with a red asterisk in the products).

The stereochemical assignments were made using NOE spectroscopy. For the keto ketal **6**, irradiation of the α -methyl group led only to enhancement of the signal for the proton at the β -position (refer to structure **8** for labels). On the other hand, irradiation of the methyl group positioned at the δ carbon led to enhancements of both the signal for the γ -H (+6.6%) as well as the H positioned at

C-2' of the sugar residue (+4%). In addition, irradiation of the signal corresponding to the anomeric H led only to enhancements of the signals for the H's positioned at carbons 3' and 5' on the sugar subunit. Clearly, these observations are consistent with our structural assignment and not the alternative diastereomer.



As anticipated, the analysis for structure **7a** was more complex. Once again, NOE experiments proved invaluable. We were also guided by NMR chemical shift analysis resulting from a B3LYP/6-31G(d) calculation carried out on structures **7a** and **7c** (Table 1).¹⁹ Irradiation of the signal for H-5' led to a 3.1% increase in the signal corresponding to H-7, suggesting that they are on the same side of the structure; in **7c**, they are on opposite sides and an enhancement would not be observed. In addition, irradiation of H-1' led to a dramatic 13.6% increase in the signal corresponding to H-2' but no effect on the signal for H-7. If the isolated material corresponded to **7c** one would have anticipated seeing a change in the signal for H-7 since in that structure, they are positioned on the same side.

Table 1
Chemical shift data for selected protons and results of NOE experiments

Structure	Calculated/observed chemical shift (δ) for proton listed below			
	H ₇	H _{2'}	H _{5'}	H _{1'}
7a	3.38/3.03	4.34/4.58	3.95/4.14	6.15/6.04
7c	2.71/—	4.31/—	4.21/—	6.15/—

—=not observed; irradiation of H₁ leads to a 13.6 enhancement of the signal for H₂; irradiation of H₁ increases the signal for H₇ by 3.1%.

2.3. A brief assessment of bioactivity

We wondered whether **7b**, the keto ketal resulting from removal of the isopropylidene group from **7a** would display any of the bioactivity that is characteristic of the pseudopterosins. Like other pseudopterosins, **7b** displayed 65% inhibition of mouse ear edema that was induced by treatment of the ear with phorbol myristate

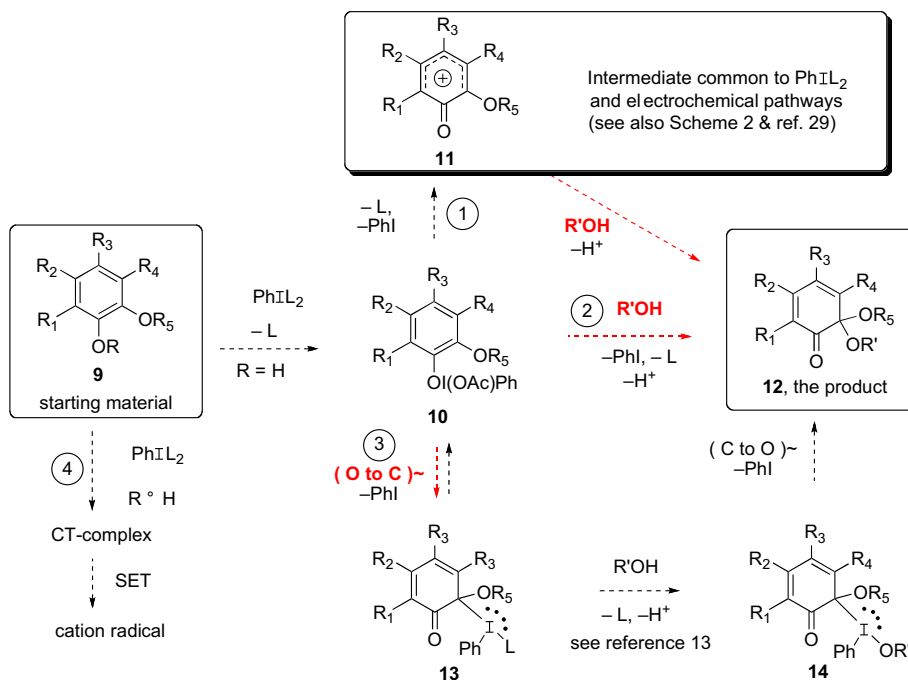
acetate. For comparison, the same amount (50 $\mu\text{g}/\text{ear}$) of pseudopterosin A (PsA, **1a**) displayed inhibition at the 84% level and afforded an ED₅₀ of 8 $\mu\text{g}/\text{ear}$ when a dose dependent evaluation was performed.²⁰ The ED₅₀ for iso-PsE (**2**) is slightly larger, being 27 $\mu\text{g}/\text{ear}$;¹² the ED₅₀ for **7b** has not yet been measured.

2.4. Mechanism

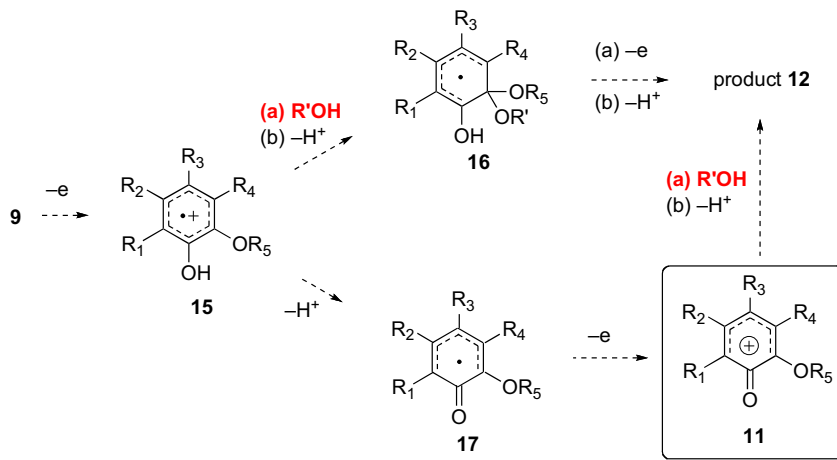
What is the mechanism for the conversion of **4–6**, and **5–7a**? Elegant studies have been conducted in both the electrochemical and reagent promoted arenas. A recent review by Quideau and co-workers summarizes their research involving each approach and also provides an excellent summary of literature citations to the work of others.¹³ In addition, we draw attention to the pioneering electrochemical research from the laboratories of Miller,²¹ Swenton,²² Yamamura,²³ Nishiyama,²⁴ Schäfer,²⁵ Dryhurst,²⁶ Hammerich and Parker,²⁷ and Nematollahi.²⁸

When PhIL₂ is utilized, literature precedence implicates the four mechanistic options illustrated in Scheme 1. Three of the pathways begin with a ligand exchange of trifluoroacetate/acetate/acetate for ArO to afford structure **10**. From there the paths diverge, one leading to the pentadienyl cation **11** via the loss of PhI and trifluoroacetate/acetate. Subsequent attack by R'OH and loss of a proton leads to the product, keto ketal **12**.²⁹ Pathway two proceeds via attack by R'OH at the OR₅-bearing carbon of **10** with concomitant displacement of PhI and trifluoroacetate/acetate to afford product **12**. A third option suggests the equilibration of **10** via a migration of iodine from oxygen to the adjacent carbon to afford the structure **13**.^{13a} Attack of R'OH upon iodine leading to **14**, followed by a carbon to oxygen migration with loss of PhI, would generate the product. Finally, for non-phenolic structures, i.e., those where R \neq H in **9**, a charge transfer (CT) complex is implicated by UV spectroscopy; a subsequent single electron transfer (SET) affords a cation radical whose existence is supported by its ESR spectrum (note pathway 4).³⁰

Electrochemically, there are two reasonable pathways to consider for transformations conducted under neutral or non-basic conditions (note Scheme 2). Each begins with a one-electron oxidation to afford cation radical **15**, an event that generally occurs in the potential range of +1 to +1.4 V.¹³ Capture of **15** by a nucleophile, R'OH, followed by the sequential loss a proton, a second electron, and a second proton leads to the product, **12**. The second pathway differs in the timing of the events, suggesting instead that the initially formed cation radical **15** undergoes the loss of a proton to afford radical **17** at a rate that exceeds capture by R'OH, and that the reaction with the latter is delayed until the penultimate stage of the 5 step sequence. Following this scenario, the radical **17** will undergo oxidation at or below the potential needed for the first oxidation step, and deliver the pentadienyl cation **11**, an intermediate that is common to both the PhIL₂ and electrochemical routes (compare Schemes 1 and 2). Subsequent capture by R'OH and proton loss delivers the product. Using symbolism that is common to electrochemical parlance, the first pathway is illustrative of an ECPEP pathway, while the second is representative of an EPECP path. In each instance, the symbols 'E', 'P', and 'C' refer to an electrochemical step, the loss (or addition) of a proton, and a chemical transformation, respectively.



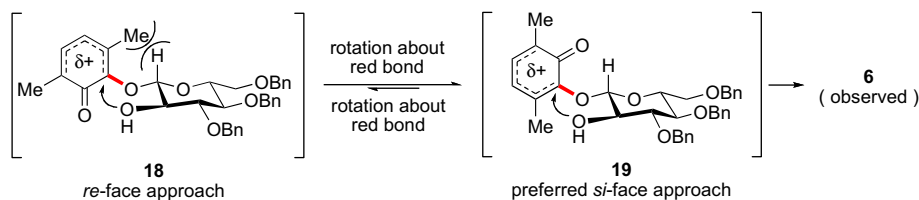
Scheme 1. Mechanistic options when $PhIL_2$ is used as an oxidant. Here and in Scheme 2, possible stereochemistry-determining steps are highlighted in red.^{13a,29}



Scheme 2. Electrochemical options: the ECPEP and EPECp pathways.

2.5. Origin of the stereoselectivity^{13,29}

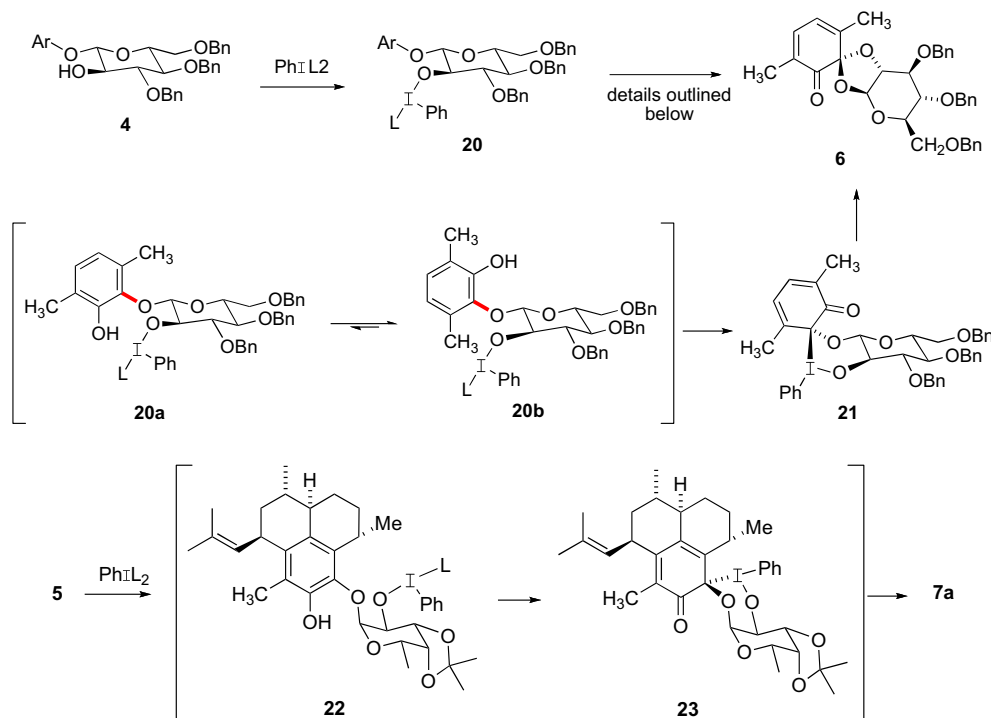
Since pentadienyl cation **11** is common to both the $PhIL_2$ and the electrochemically promoted pathways shown in Schemes 1 and 2, we begin our discussion focusing upon this type of intermediate. In the transition structure for the model system **4**,



attack upon the *re*-face suffers from an energy raising interaction between the anomeric hydrogen and one of the two methyl groups appended to the catechol framework, as exemplified by structure **18**. That interaction is replaced by a less demanding one between the anomeric hydrogen and the carbonyl unit when the

si-face is approached in the manner portrayed by structure **19**. Thus, subject to the condition that attack upon a pentadienyl cation intermediate is stereochemically determining, we predict that keto ketal **6** will be the preferred product derived from both the $PhIL_2$ and electrochemically promoted paths, and this is observed.

An alternative hypothesis, one that is similar to the third pathway shown in Scheme 1 and is consistent with a recent model put forth by Quideau and co-workers,^{13,31} It capitalizes upon the chirality that is present in the sugar portion of the starting material. As portrayed in Scheme 3, the sequence begins with a reaction by the C-2' hydroxyl



Scheme 3. Alternative mechanistic rationale.

group of the sugar with PhIL_2 to form the λ^3 -iodane structures **20a,b**. Intramolecular cyclization with displacement of the second trifluoroacetate/acetate ligand leads to a cyclic structure represented by **21**. Migration of oxygen from iodine to carbon with the concomitant loss of iodobenzene, leads to the observed product, **6**. Application of the same line of reasoning to the iso-PsE derived substrate **5** leads to the analysis shown in Scheme 3, and the prediction that the observed product, **7a**, ought to be preferred.

2.6. Commentary regarding possible bio-relevance

We close our discussion with commentary regarding the possible relevance of the electron transfer chemistry discussed herein to the bioactivity expressed by the pseudopterosins. Not long ago we determined that the pseudopterosins target the adenosine class of G-protein coupled receptors (GPCR).³² In general, their activation is triggered by a conformational change that is induced by the guest, in the present case, a pseudopterosin.^{32c} We speculate that the conformational change that accompanies the cyclization of **24–25** could trigger a conformational change in the receptor that sets in motion a cascade of events that ultimately leads to the expression of pseudopterosin bioactivity.³³ That **24** could be formed via electron transfer and acid–base reactions that are common in biological systems, is in accord with this description and is an attractive feature of this proposal. The reversibility of each of step is another attractive element since this provides a means of re-establishing the receptor's resting state.

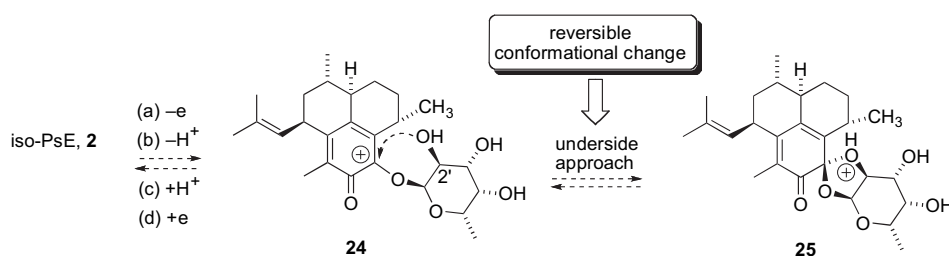
3. Concluding remarks

In conclusion, we have shown that pseudopterosin oxidation leads to the formation of a keto ketal that is formed via intramolecular trapping by the hydroxyl group positioned at C-2' of the pendant sugar. The keto ketal displays anti-inflammatory activity, albeit to a lesser degree than the natural products. Accompanying the cyclization is a conformational change that may trigger the activation/deactivation of adenosine receptors with which the pseudopterosins are known to interact. Additional experiments are needed to address this hypothesis; they are currently underway.

4. Experimental section

4.1. General

4.1.1. Compound 4. To a solution of tri-*O*-benzyl glucal (0.28 g, 0.67 mmol) in dry DCM (10 mL) at 0 °C was added freshly prepared DMDO in acetone (9.6 mL, 0.07 mol/L) dropwise. The reaction mixture was stirred at 0 °C for 10 min and then flushed using dry argon. The resulting white solid was dissolved in dry acetone (4.5 mL) and then added to a refluxing solution of 3,6-dimethyl catechol (372 mg, 2.69 mmol), K_2CO_3 (745 mg, 5.39 mmol) and catalytic amount of 18-crown-6 (3 mg) in dry acetone (11.5 mL). The reaction mixture was refluxed for 3 h, and then cooled to room temperature. The solution was filtered through a pad of Celite, and



then concentrated to dryness in vacuo. The residue was dissolved in ethyl acetate (20 mL) and poured into 1 N HCl (20 mL). The aqueous layer was extracted with ethyl acetate (2×10 mL). The combined extracts were washed with brine (40 mL), dried over Na₂SO₄, filtered and then concentrated to dryness in vacuo. The residue was purified by column chromatography over silica gel (toluene/acetone, 100:1, v/v) to afford aryl O-glycoside **4** (0.25 g, 0.44 mmol, 65%) as an orange oil. *R*_f 0.29 (hexane/ethyl acetate, 9:1, v/v). ¹H NMR (CDCl₃, 200 MHz): δ 7.57 (br, 1H), 7.27–7.09 (m, 15H), 6.76 (d, 1H, *J*=7.8), 6.51 (d, 1H, *J*=7.8), 4.87 (d, 1H, *J*=11.4), 4.76 (d, 1H, *J*=10.8), 4.74 (d, 1H, *J*=11.4), 4.54 (d, 1H, *J*=10.8), 4.50–4.41 (m, 3H), 3.77–3.43 (m, 5H), 3.38–3.31 (m, 1H), 2.97 (br, 1H), 2.23 (s, 3H), 2.13 (s, 3H). ¹³C NMR (CDCl₃, 50 MHz): δ 147.6, 143.2, 138.2, 137.9, 137.7, 129.2, 128.6, 128.4, 128.3, 127.9, 127.7, 126.9, 123.6, 120.7, 105.3, 84.4, 77.3, 75.3, 74.9, 74.2, 73.5, 68.3, 16.5, 15.8. ESI-MS: found 593.2523, C₃₅H₃₈O₇Na⁺ Calculated 593.2515.

4.1.2. Compound 6. To a solution of PIDA (0.24 g, 0.75 mmol) in dry CH₃NO₂ (50 mL) at 0 °C was added TFA (87 μL, 1.13 mmol), followed by addition of a solution of compound **4** (284 mg, 0.5 mmol) in dry DCM (50 mL). The resulting solution was stirred at 0 °C for 30 min, and then quenched by solid NaHCO₃ (2.5 g). The solution was filtered through a pad of Celite, and then concentrated to dryness in vacuo. The residue was purified by column chromatography over silica gel (hexane/ethyl acetate/TEA, 95/5/0.5, v/v/v) to afford compound **6** (181 mg, 0.32 mmol, 64%) as a yellow oil. *R*_f 0.51 (hexane/ethyl acetate, 5:1, v/v). ¹H NMR (CDCl₃, 200 MHz): δ 7.28–7.06 (m, 15H), 6.58 (d, 1H, *J*=6.4), 5.92 (d, 1H, *J*=6.4), 5.27 (d, 1H, *J*=7.2), 4.86 (d, 1H, *J*=10.8), 4.82 (d, 1H, *J*=11.6), 4.63 (d, 1H, *J*=11.6), 4.59 (d, 1H, *J*=12.0), 4.45–4.39 (m, 2H), 4.01–3.93 (m, 1H), 3.69–3.52 (m, 5H), 1.93 (s, 3H), 1.79 (s, 3H). ¹³C NMR (CDCl₃, 50 MHz): δ 197.8, 144.1, 138.1, 137.9, 137.8, 137.3, 130.2, 128.3, 127.9, 127.8, 127.7, 127.6, 123.4, 100.3, 100.1, 94.4, 82.4, 81.6, 78.2, 77.4, 75.2, 73.4, 72.8, 68.4, 17.2, 14.7. ESI-MS: found 591.2368, C₃₅H₃₆O₇Na⁺ Calculated 591.2359.

4.1.3. Compound 5. To a solution of iso-PsE (115 mg, 0.26 mmol) in dry acetone (0.55 mL) was added 2,2-dimethoxypropane (0.55 mL) and a catalytic amount of p-TsOH (5 mg). The reaction mixture was stirred at room temperature for 14 h and then quenched using TEA (25 μL). The mixture was concentrated to dryness in vacuo. The residue was purified by column chromatography over silica gel (hexane/ethyl acetate, 10/1, v/v) to afford compound **5** (102 mg, 0.21 mmol, 82%) as a white solid. *R*_f 0.48 (hexane/ethyl acetate, 5:1, v/v). ¹H NMR (CDCl₃, 200 MHz): δ 8.11 (br, 1H), 5.15–5.08 (m, 2H), 4.69–4.58 (m, 1H), 4.50 (t, 1H, *J*=6.2), 4.23 (dd, 1H, *J*=2.2, 6.2), 4.09 (m, 1H), 3.65 (m, 1H), 3.47–3.37 (m, 2H), 2.24–1.97 (m, 6H), 1.76 (d, 3H, *J*=1.2), 1.69 (d, 3H, *J*=1.2), 1.65–1.54 (m, 4H), 1.50 (s, 3H), 1.39 (m, 6H), 1.20 (d, 1H, *J*=7.2), 1.06 (d, 1H, *J*=5.6). ¹³C NMR (CDCl₃, 50 MHz): δ 145.3, 141.9, 135.2, 133.1, 129.8, 128.4, 121.5, 109.7, 101.9, 75.5, 75.3, 69.9, 65.4, 41.9, 39.4, 35.6, 30.4, 29.5, 27.7, 26.9, 25.8, 25.6, 23.6, 20.9, 17.6, 16.4, 10.8. ESI-MS: found 509.2886, C₂₉H₄₂O₆Na⁺ Calculated 509.2879.

4.1.4. Compound 7a. To a solution of PIDA (86 mg, 0.27 mmol) in dry CH₃NO₂ (18 mL) at 0 °C was added TFA (31 μL, 0.40 mmol), followed by addition of a solution of compound **5** (86 mg, 0.18 mmol) in dry DCM (18 mL). The resulting solution was stirred at 0 °C for 30 min, and then quenched by solid NaHCO₃ (885 mg). The solution was filtered through a pad of Celite, and then concentrated to dryness in vacuo. The residue was purified by column chromatography over silica gel (hexane/ethyl acetate/TEA, 95/5/0.5, v/v/v) to afford compound **7a** (48 mg, 0.099 mmol, 56%) as a yellow oil. *R*_f 0.48 (hexane/ethyl acetate/TEA, 10:1:0.05, v/v/v). ¹H NMR (CDCl₃, 200 MHz): δ 6.04 (d, 1H, *J*=5.8), 5.03 (m, 1H), 4.59–4.51 (m, 2H), 4.16–4.05 (m, 2H), 3.55 (d, 1H, *J*=9.4), 3.03 (m, 1H), 2.24–2.05

(m, 2H), 1.91–1.80 (m, 1H), 1.74–1.68 (m, 8H), 1.62–1.46 (m, 7H), 1.34–1.22 (m, 8H), 1.16 (d, 3H, *J*=7.2), 1.00 (d, 3H, *J*=5.2). ¹³C NMR (CDCl₃, 50 MHz): δ 198.1, 150.9, 141.6, 136.9, 132.6, 126.7, 124.7, 108.7, 98.4, 72.7, 71.8, 68.8, 63.2, 40.8, 38.1, 36.8, 30.3, 28.2, 27.3, 26.1, 25.6, 24.4, 21.0, 19.5, 17.6, 15.9, 9.9. ESI-MS: found 507.2731, C₂₉H₄₀O₆Na⁺ Calculated 507.2722.

4.1.5. Compound 7b. To a solution of iso-PsE (75 mg, 0.17 mmol) in dry DCM (2 mL) was added *p*-methoxybenzaldehyde dimethyl acetal (0.26 mL) and catalytic amount of CSA (8 mg). The reaction mixture was stirred at room temperature for 24 h and then quenched by TEA (25 μL). The mixture was concentrated to dryness in vacuo. The residue was purified by column chromatography over silica gel (hexane/ethyl acetate, 10/1, v/v) to afford PMB protected iso-PsE (67 mg, 0.12 mmol, 71%) as a yellow oil. To a solution of PIDA (59 mg, 0.18 mmol) in dry CH₃NO₂ (12 mL) at 0 °C was added TFA (23 μL, 0.3 mmol), followed by addition of a solution of PMB protected iso-PsE (67 mg, 0.12 mmol) in dry DCM (12 mL). The resulting solution was stirred at 0 °C for 30 min, and then quenched by solid NaHCO₃ (595 mg). The solution was filtered through a pad of Celite, and then concentrated to dryness in vacuo. The residue was purified by column chromatography over silica gel (hexane/ethyl acetate/TEA, 95/5/0.5, v/v/v) to afford keto ketal (36 mg, 0.064 mmol, 54%) as a yellow solid. To a solution of PMB protected keto ketal (36 mg, 0.064 mmol) in DCM/H₂O (1.26 mL, 17/1, v/v) was added DDQ (39 mg, 0.13 mmol) at room temperature. The reaction mixture was stirred at room temperature for 4 h, and then diluted with DCM (2 mL) followed by filtered through Celite. The organic layer was washed with satd NaHCO₃ (2 mL), dried over Na₂SO₄, filtered and then concentrated to dryness in vacuo. To a solution of the residue in DCM/MeOH (1.2 mL, 1:1, v/v) was added NaOMe (pH=8–10). The reaction mixture was stirred at room temperature for 12 h, and then concentrated to dryness in vacuo. The residue was purified by column chromatography over silica gel (DCM/MeOH/TEA, 100/1/0.5, v/v/v) to afford compound **7b** (18 mg, 0.04 mmol, 63%) as a yellow oil. *R*_f 0.32 (DCM/MeOH, 50:1, v/v). ¹H NMR (CDCl₃, 200 MHz): δ 6.02 (d, 1H, *J*=5.6), 5.06 (m, 1H), 4.53 (t, 1H, *J*=4.8, 5.6), 4.24–3.97 (m, 2H), 3.96–3.71 (m, 4H), 3.61–3.47 (m, 2H), 2.78 (m, 1H), 2.13 (m, 1H), 1.78 (m, 2H), 1.70–1.41 (m, 9H), 1.38 (d, 1H, *J*=6.6), 1.30–1.23 (m, 4H), 1.20 (d, 3H, *J*=7.2), 1.00 (d, 3H, *J*=6.0), 0.91 (m, 1H). ¹³C NMR (CDCl₃, 100 MHz): δ 197.9, 151.7, 142.3, 135.9, 132.5, 126.0, 124.6, 97.7, 77.2, 73.3, 69.0, 68.3, 64.7, 40.8, 38.1, 36.9, 30.4, 28.6, 28.5, 26.3, 25.7, 21.1, 19.7, 17.6, 16.4, 9.7. ESI-MS: found 467.2419, C₂₆H₃₆O₆Na⁺ Calculated 467.2410.

Acknowledgements

We gratefully acknowledge the U.S. Army Medical Research Program (Grant Number W81XWH-06-1-0089) for its support of this research. The Supported Activity was also sponsored, in part, by an educational donation provided by Amgen. The authors are grateful to them.

We are appreciative of the efforts of Mr. Ian Pahk who synthesized 3,6-dimethyl catechol, and Mr. Abdul Hackim for performing the CV experiments on the resulting model system, **4**.

References and notes

- Look, S. A.; Fenical, W.; Matsumoto, G. K.; Clardy, J. *J. Org. Chem.* **1986**, *51*, 5140–5145.
- Roussis, V.; Wu, Z.; Fenical, W.; Strobel, S. A.; Van Duyne, G. D.; Clardy, J. *J. Org. Chem.* **1990**, *55*, 4916–4922.
- (a) Ata, A.; Kerr, R. G.; Moya, C. E.; Jacobs, R. S. *Tetrahedron* **2003**, *59*, 4215–4222; (b) Coleman, A. C.; Kerr, R. G. *Tetrahedron* **2000**, *56*, 9569–9574.
- Look, S. A.; Fenical, W.; Jacobs, R. S.; Clardy, J. *Proc. Natl. Acad. Sci. U.S.A.* **1986**, *83*, 6238–6240.
- Ettouati, W.; Jacobs, R. S. *Mol. Pharmacol.* **1987**, *31*, 500–505.

6. Mayer, M. S. A.; Jacobson, P. B.; Fenical, W.; Jacobs, R. S.; Glaser, K. B. *Pharm. Lett.* **1998**, *62*, 401–407.
7. Moya, C. E.; Jacobs, R. S. *Comp. Biochem. Physiol. C, Pharmacol. Toxicol.* **2006**, *143*, 436–443.
8. Haimes, H.; Glasson, S.; Harlan, P.; Jacobs, R.; Fenical, W.; Jimenez, J. *Inflamm. Res.* **1995**, *44*, 13–17.
9. Montesinos, M. C.; Gadangi, P.; Longaker, M.; Sung, J.; Levine, J.; Nilsen, D.; Reibman, J.; Li, M.; Jiang, C.-K.; Hirschhorn, R.; Recht, P. A.; Ostad, E.; Levin, R. I.; Cronstein, B. N. *J. Exp. Med.* **1997**, *186*, 1615–1620.
10. (a) Harrowven, D. C.; Tyte, M. J. *Tetrahedron Lett.* **2004**, *45*, 2089–2091; (b) Kocienski, P. J.; Pontiroli, A.; Qun, L. *J. Chem. Soc., Perkin Trans. 1* **2001**, 2356–2366; (c) Chow, R.; Kocienski, P. J.; Kuhl, A.; LeBrazidec, J.-Y.; Muir, K.; Fish, P. *J. Chem. Soc., Perkin Trans. 1* **2001**, 2344–2355; (d) Lazerwith, S. E.; Johnson, T. W.; Corey, E. J. *Org. Lett.* **2000**, *2*, 2389–2392; (e) Benoit-Marquie, F.; Csaky, A. G.; Esteban, G.; Martinez, M. E.; Plumet, J. *Tetrahedron Lett.* **2000**, *41*, 3355–3358; (f) Corey, E. J.; Lazerwith, S. E. *J. Am. Chem. Soc.* **1998**, *120*, 12777–12782; (g) LeBrazidec, J.-Y.; Kocienski, P. J.; Connolly, J. D.; Muir, K. W. *J. Chem. Soc., Perkin Trans. 1* **1998**, 2475–2478; (h) Geller, T.; Jakupovic, J.; Schmalz, H.-G. *Tetrahedron Lett.* **1998**, *39*, 1541–1544; (i) Majdalani, A.; Schmalz, Hans G. *Synlett* **1997**, 1303–1305; (j) Buszek, K. R.; Bixby, D. L. *Tetrahedron Lett.* **1995**, *36*, 9129–9132; (k) Harrowven, D. C.; Dennison, S. T.; Howes, P. *Tetrahedron Lett.* **1994**, *35*, 4243–4246; (l) Jung, M. E.; Siedem, C. S. *J. Am. Chem. Soc.* **1993**, *115*, 3822–3823; (m) Kozikowski, A. P.; Wu, J. P. *Synlett* **1991**, 465–468; (n) McCombie, S. W.; Cox, B.; Ganguly, A. K. *Tetrahedron Lett.* **1991**, *32*, 2087–2090; (o) Ganguly, A. K.; McCombie, S. W.; Cox, B.; Lin, S.; McPhail, A. T. *Pure Appl. Chem.* **1990**, *62*, 1289–1291; (p) Corey, E. J.; Carpino, P. *Tetrahedron Lett.* **1990**, *31*, 3857–3858; (q) Corey, E. J.; Carpino, P. *J. Am. Chem. Soc.* **1989**, *111*, 5472–5474; (r) Broka, C. A.; Chan, S.; Peterson, B. *J. Org. Chem.* **1988**, *53*, 1584–1586.
11. Perez Gonzalez, M.; Teran, C.; Teixeira, M. *Med. Res. Rev.* **2008**, *28*, 239–371; Jacobson, K.; Gao, Z. *Nat. Rev.* **2006**, *5*, 247–264.
12. Hoarau, C.; Day, D.; Moya, C.; Wu, G.; Hackim, A.; Jacobs, R. S.; Little, R. D. *Tetrahedron Lett.* **2008**, *49*, 4604–4606.
13. (a) Quideau, S.; Pouysegue, L.; Deffieux, D. *Synlett* **2008**, 467–495 and references therein; (b) Torii, S. *Electro-organic Syntheses, Methods and Applications; Part I: Oxidations*; Kodansha, VCH: Tokyo, 1985; Chapter 4; (c) Morrow, G. W. Anodic oxidation of oxygen-containing compounds In *Organic Electrochemistry*; Lund, H., Hammerich, O., Eds.; Dekker: New York, NY, 2001; Chapter 16; (d) Yoshida, K. *Electrooxidation in Organic Chemistry: The Role of Cation Radicals as Synthetic Intermediates*; Wiley Interscience: New York, NY, 1984; (e) Chum, H. L.; Baizer, M. M. *The Electrochemistry of Biomass Derived Materials* ACS Monograph Series 183; American Chemical Society: Washington, DC, 1985; (f) Eickhoff, H.; Jung, G.; Rieker, A. *Tetrahedron* **2001**, *57*, 353–364.
14. For additional examples, refer to: (a) Park, Y. S.; Wang, S.; Tantillo, D.; Little, R. D. *J. Org. Chem.* **2007**, *72*, 4351–4357; (b) Miranda, J.; Wade, C.; Little, R. D. *J. Org. Chem.* **2005**, *70*, 8017–8026.
15. The difference in peak potentials as well as the differing shapes of the CV curves for the two systems can, in principle, be attributed to any of a number of factors. Since the potentials differ by only ca. 100 mV, caution must be exercised. Whichever interpretation one elects to use must be guided by the elegant studies recently described by Merkel, P. B.; Luo, P.; Dinnocenzo, J. P.; Farid, S. *J. Org. Chem.* **2009**, *74*, 5163–5173. We are grateful to a reviewer for calling our attention to this reference.
16. (a) Moeller, K. D.; Tinai, L. V. *J. Am. Chem. Soc.* **1992**, *114*, 1033–1041; (b) Fry, A. J. *Synthetic Organic Electrochemistry*, 2nd ed.; Wiley & Sons: New York, NY, 1989; Chapters 2 and 3.
17. (a) Zhdankin, V. V.; Stang, P. J. *Chem. Rev.* **2008**, *108*, 5299–5358; (b) Quideau, S.; Feldman, K. S. *Tetrahedron* **2001**, *57*, ix–x with the entire issue, pages 265–423 dealing with the topic 'Oxidative activation of aromatic rings: an efficient strategy for arene functionalization'.
18. (a) Magdziak, D.; Meek, S. J.; Pettus, T. R. *Chem. Rev.* **2004**, *104*, 1383–1430; (b) Liang, H.; Ciufolini, M. A. *J. Org. Chem.* **2008**, *73*, 4299–4301.
19. Interestingly, since the observed product **7a** is calculated to be 2 kcal/mol lower in energy than **7c** in the gas phase and ~2.16 kcal/mol lower in water, the absence of **7c** may reflect a thermodynamic rather than a kinetic preference. Calculations were conducted using Spartan 08 for Macintosh.
20. We thank Dr. Claudia Moya of the Department of Ecology, Evolution, and Marine Biology for conducting this experiment. Additional detail concerning the pharmacology will be reported on another occasion.
21. Miller, L. L.; Stermitz, F. R.; Falck, J. R. *J. Am. Chem. Soc.* **1973**, *95*, 2651–2656.
22. (a) Swenton, J. S.; Callinan, A.; Chen, Y.; Rohde, J. J.; Kerns, M. L.; Morrow, G. W. *J. Org. Chem.* **1996**, *61*, 1267–1274; (b) Swenton, J. S. *Acc. Chem. Res.* **1983**, *16*, 74–81.
23. Yamamura, S.; Nishiyama, S. *Synlett* **2002**, 533–543.
24. Amano, Y.; Nishiyama, S. *Tetrahedron Lett.* **2006**, *47*, 6505–6507.
25. Klunenberger, H.; Schaeffer, C.; Schäfer, H. *J. Tetrahedron Lett.* **1982**, *23*, 4581–4584.
26. Shen, X.-M.; Dryhurst, G. *Tetrahedron* **2001**, *57*, 393–405.
27. Hammerich, O.; Parker, V. D. *Acta Chem. Scand.* **1982**, *B36*, 63–64.
28. (a) Raoof, J.-B.; Ojani, R.; Nematollahi, D.; Kiani, A. *Internat. J. Electrochem. Sci.* **2009**, *4*, 810–819; (b) Nematollahi, D.; Khoshafar, H. *Tetrahedron* **2009**, *65*, 4742–4750; (c) Rafiee, M.; Nematollahi, D. *J. Electroanal. Chem.* **2009**, *626*, 36–41; Nematollahi, D.; Dehdashtian, S.; Niazi, A. *J. Electroanal. Chem.* **2008**, *616*, 79–86.
29. (a) Kurti, L.; Herczegh, P.; Visy, J.; Simonyi, M.; Antus, S.; Pelter, A. *J. Chem. Soc., Perkin Trans. 1* **1999**, 379–380; (b) Venkateswarlu, R.; Kamakshi, C.; Subhash, P. V.; Moinuddin, S. G. A.; Reddy, D. R. S.; Ward, R. S.; Pelter, A.; Gelbrich, T.; Hursthouse, M. B.; Coles, S. J.; Light, M. E. *Tetrahedron* **2006**, *62*, 4463–4473; (c) Pelter, A.; Ward, R. S. *Tetrahedron* **2001**, *57*, 273–282.
30. (a) Kita, Y.; Fujioka, H. *Pure Appl. Chem.* **2007**, *79*, 701–713; (b) Hata, K.; Hamamoto, H.; Shiozaki, Y.; Caemmerer, S. B.; Kita, Y. *Tetrahedron* **2007**, *63*, 4052–4060; (c) Kita, Y.; Takada, T.; Tohma, H. *Pure Appl. Chem.* **1996**, *68*, 627–630; (d) Kita, Y.; Tohma, H.; Hatanaka, K.; Takada, T.; Fujita, S.; Mitoh, S.; Sakurai, H.; Oka, S. *J. Am. Chem. Soc.* **1994**, *116*, 3684–3691.
31. Pouysegue, L.; Chassaing, S.; Dejuguac, D.; Lamidey, A.-M.; Miqueu, K.; Sotiropoulos, J.-M.; Quideau, S. *Angew. Chem., Int. Ed.* **2008**, *47*, 3552–3555.
32. (a) Tanis, V. M.; Moya, C.; Jacobs, R. S.; Little, R. D. *Tetrahedron* **2008**, *64*, 10649–10663; (b) Zhong, W.; Moya, C.; Jacobs, R. S.; Little, R. D. *J. Org. Chem.* **2008**, *73*, 7011–7016; (c) Thus far our binding studies reveal cooperative binding of PsA to the adenosine A_{2A} and A₃ receptors.
33. Henchman, R. H.; Wang, H.-L.; Sine, S. M.; Taylor, P.; McCammon, J. A. *Biophys. J.* **2006**, *88*, 2564–2576.